# Numerical Modeling of Bio-Kinetic Chains in a 5m Penalty Shot in Men's Elite Water-polo

B. Zepeda-Almazan[1]

SID: 29001480

[1]Sheffield Hallam University | MSc Sports Engineering

Submitted on Dec $9^{th}$, 2019.

## Abstract

**Context:** Using MATLAB software to investigate interactions of bio-kinetic chain movements of elite water-polo athletes to determine resultant trajectory and reaction-time in a 5m penalty shot during competitive play.

**Aims:** Current research shows launch velocity of a short-range water-polo shot is highly dependent on anatomical twist and extension angle of kinetic-chain members such as the torso and upper-arm respectively.

## 1 Introduction & Background

Invented in the 19th Century, water-polo has evolved into a power and endurance-based sport that combines techniques found in sports such as baseball, rugby and football. Points are earned by throwing the ball into the opposing goal during normal play as well as earned penalty shots, as seen in football. The fastest recorded penalty shot is 26.8 $ms^{-1}$ by a Turkish national team male; 5.7 $ms^{-1}$ faster than the average elite male water-polo player (Solum, 2017). This equates to 0.186 s for the defending goalie to react and stop the ball. As the average reaction time (RT) of an elite water-polo male is 0.213s (Gardasevic et al.,2019) this would require preemptive perception and leave little time for a successful defensive play.

Numerous studies have supported the positive relationship between certain components of a shooter's technique and launch velocity (Razak et al., 2018). Solum (2017) quantified the torso as producing 25% of the total force in ball launch velocity. Melchiorri et al. (2011) suggested a positive relationship to trunk rotation time and ball velocity through a study of the Italian men's National team. These studies support the findings of Feltner & Nelson (1996) who used direct linear transformation (DLT) via planar images to quantify the contributions of anatomical kinetic chains towards the ball release velocity. It was determined the key contributing factors were the trunk twist (24.2%), rotation of the upper arm (13.2%), forearm extension (26.6%), and the relative velocity of the ball to center of hand (10.4%), totaling 75% of all velocity contributions from 14 observed components. These findings were adapted to formulate a numerical model that receives user input for initial launch conditions to plot a trajectory, and subsequently calculate total time per penalty shot, otherwise referred to as RT. This information may provide insightful intelligence to aid water-polo players and coaches in determining strategic trajectories and appropriate training techniques.

### 1.1 Assumptions

The model operates on certain assumptions representing standard environmental (air/water density, water surface tension) and player physical metrics (anatomical dimensions, performance rotational momentum) during an elite water-polo match. Melchiorri et al. (2011) concluded that initial vertical displacement and rotation of the shoulders did not correlate to final launch velocity and are therefore kept constant at experimental mean values. Resistance due to airborne water drag are neglected, as the ball is assumed to be thrown in dry. The equations used to determine the lift/spin impacts of the ball are deemed to satisfy a ball that is *gravity driven* as determined by Dupeux et al. (2010).

$$7\,\bar{\bar{\rho}}R \gg \frac{U_0^2}{g} \tag{1}$$

Gravity dependent balls such as water-polo balls, basketballs and handballs experience limited aerodynamic influence from drag and lift forces outside of parabolic trajectory (Dupeux et al. 2010). Clanet (2015) characterized lateral deviations as a sinusoidal approximation that assumes a wavelength (Equation 20) that must be satisfied to witness lateral deviation. The 5m distance is significantly less than the approximated wavelength of 27m which limits the visibility of lift or spin induced lateral deviations. Due to short trajectory distance, the Reynolds Value is constant (Clanet, 2015).

$$Re = \frac{2RU_\infty}{v} = 6 \times (10)^5 \tag{2}$$

### 1.2 Horizontal & Vertical Force Components

The horizontal forces affecting the ball's trajectory are presented in Figure 1. The Lift and Drag forces are referenced from Haake, Goodwil, & Carre (2007) where the general equations represent a sports ball travelling through a medium with density ρ. Initial components of the launch force are measured by crossing the angular velocities of respective anatomic kinetic members and unit vectors (Figure 1).

$$x = x_{(n-1)} + v_{x(n-1)}\Delta t \tag{3}$$

$$v_x = v_{x(n-1)} + dv_{x(n-1)}\Delta t \tag{4}$$

$$dv_x = \frac{\left(-F_{D(n)} * cos\alpha_n\right) - \left(F_{L(n)} * sin\alpha_n\right)}{M} \tag{5}$$

The vertical components are a sum of initial launch conditions $(v_1, \alpha, \phi)$ as well as drag and lift forces.

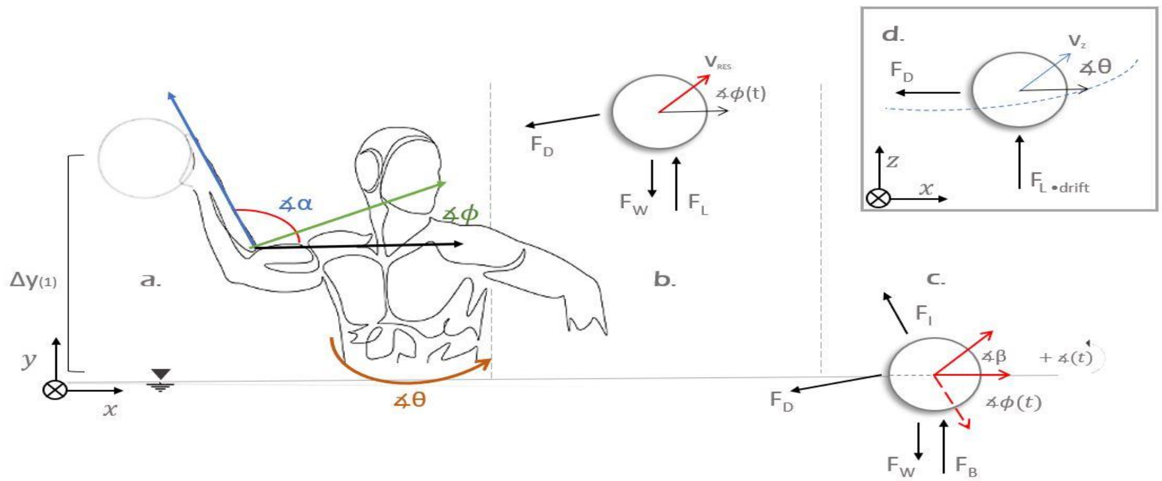


**Figure 1** Free Body Diagram of three trajectory phases || a. Shot Preparation, b. Airborne, c. Skipping (short shot/contact with water) ||

$$y = y_{(n-1)} + v_{y(n-1)}\Delta t \quad (6)$$

$$v_y = v_{y(n-1)} + dv_{y(n-1)}\Delta t \quad (7)$$

$$dv_y = \frac{\left(-F_{D(n)} * cos\alpha_n\right) - \left(F_{L(n)} * sin\alpha_n\right)}{m} \quad (8)$$

$$F_{D(n)} = 0.5A\rho_{air}v_{res(n)}^2 * c_{d(n)} \quad (9)$$

$$F_{L(n)} = 0.5A\rho_{air}v_{res(n)}^2 * c_{l(n)} \quad (10)$$

## 1.3 Water impact for bouncing

The player can either execute a lob, in which the ball does not interact with the water, or a skip shot, in which the ball is bounced on the water's surface to add a dynamic path to deceive the goalie.

Johnson & Reid (1975) derived characteristic equations to define the projectile motion of a sphere hitting water which leads to three behaviors: ricochet, skipping, and broaching. These equations are complemented by those derived by Beldan et al. (2015) who used slow motion capture to investigate skipping regimes of spheres upon impact. This model observes ricocheting and skipping but will abstain from recognizing broaching phenomena due to a lack of application purposes in this sport. The derived critical angle (Equation 11) represents the angle threshold to initialize either of these movements. An angle larger than $\theta_c$ will result in an oscillating submersion until settling at the surface. This equation is a simplified version of the proposed equations from Birkhoff et al. (1944) while still supporting the conclusive characterization of projectile motion upon surface impact.

$$\theta_c = \frac{18^\circ}{\sqrt{\frac{\rho_b}{\rho_{air}}}} \quad (11)$$

$$F_I = \frac{3\lambda v_{y(i)}^2 8\pi R}{\left(\frac{\rho_w}{\rho_b}\right)\sin(45^\circ - \alpha_i)\cos(\alpha_i)} \quad (12)$$

## 1.4 Lateral Force Components

The Z direction is directly impacted by over rotation of the torso from the central axis of 0° measured from the sagittal plane when hips are squared to goal. Rotation about the sagittal plane is critical to trunk acceleration contribution to launch velocity, as well as where the ball will be aimed within the goal. The following equations were used to determine the movement in the lateral (z) direction:

$$z = x_{\{(n-1)\}} + v_{\{z(n-1)\}\Delta t} \quad (13)$$

$$v_z = v_{\{z(n-1)\}} + dv_{\{z(n-1)\}\Delta t} \quad (14)$$

$$dv_z = \frac{\left(-F_{D(n)} * cos\alpha_n\right) - \left(F_{L(n)} * sin\alpha_n\right)}{M} \quad (15)$$

$$c_l = 0.2 * \sin\left(2\pi f(n)\right) \quad (16)$$

$$c_d = 0.55 + \frac{1}{22.5 + \left(4.2\frac{v_{res(n)}}{v_{spin}}^{2.5}\right)^{0.4}} \quad (17)$$

Texier et al. (2016) modeled the lateral (z) movement of a ball as a sine wave with an amplitude and frequency modeled by equations 18 – 22. ( $\widetilde{C_L} = (St = 0.2)$):

$$C_{\{L(t)\}} = \int \widetilde{C_L}(f)sin(2\pi f(t) + \psi)\, df \quad (18)$$

$$f_n = \frac{0.2v_{res(n)}}{D} \quad (19)$$

$$\lambda_n = 2D\pi\sqrt{\frac{2\rho_b}{3\rho_{air}C_{Lm}}} \quad (20)$$

$$\delta_n = \left(\frac{3Dc_{(L_{(n)})}}{16\pi^2}\right)\left(\frac{\rho_{air}}{\rho_b}\right)\left(\frac{x_{(n)}}{D}\right)^2 \quad (21)$$

$$z_{drift(n)} = \delta_n sin(\lambda_n + \psi) \quad (22)$$

# 2 Model Setup

The model was created using MATLAB (R2018b) software to compare numerous outcomes varied by input values for torso rotation, $\phi$, and launch angle, α (defined by elbow flexion angle). Acceleration rates, and environmental variables were all kept constant to align with actual game play scenarios. Independent variables: elbow extension, trunk rotation, and launch angle are requested from the user via an input prompt in the launch screen. The first two rows of trajectory data are initialized based on the boundary conditions before then entering a *for loop* to calculate the full trajectory path. The data is halted at x = 5 as this represents the full 5m shot. The model calculates the final time that the goalie must react to the speed of the shot. The trajectory path(s) defined by the user is then displayed on a UI alongside an interactive legend and data summary to allow for comparison and analysis.

# 3 Results

The model outputs the results and finds that the fastest shot times are on the left side of the sagittal plane; likely due to greater torso rotation and accumulation of launch power. Figure 3 summarizes the deviation from mean RT (mean launch velocity of 21.1 $ms^{-1}$). The model validates the experimental ranges of Abraldes (2012); Mean 20.66 $ms^{-1}$ and that of Elliot & Armour (1988) 19.4 $ms^{-1}$.

## 3.1 Insights and limitations

The model allows for comparison of numerous shot trajectories to determine strategic plays. Due to user ease of use, only top contributing variables are initialized through user inputs. All others are kept constant therefore limiting accuracy to in-situ scenarios. The interactions upon impact of a ball to water surface are limited to direct ricochet and do not account for entry variables such as splashing and broaching.

This information supports the conclusion of Razak et al. (2018) who suggested specific training programs to strengthen the core muscles that impact launch velocity. Coaching staff may benefit from including such programming in their own training schedules. Goalies might gain perspective in planning defensive plays based on shooter geometry. Conversely, the shooter will be informed as to where best aim the ball along with appropriate placement of kinetic chain members to execute the shot accordingly. Suggested further work is to identify key kinetic chain wind ups in the shot process to identify projected aims/trajectory to condition the goalie in pre-emptive defense.

| 0.0 | | 0.2 | | 0.4 | | 0.6 | | 0.8 | | 1.0 | | 1.2 | | 1.4 | | 1.6 | | 1.8 | | 2.0 | | 2.2 | | 2.4 | | 2.6 | | 2.8 | | 3.0 | | 3.2 |
|---|---|---|---|---|---|---|---|---|---|---|---|---|---|---|---|---|---|---|---|---|---|---|---|---|---|---|---|---|---|---|---|---|
| | -2.6 | -2.6 | -2.5 | -2.4 | -2.4 | -2.3 | -2.2 | -2.0 | -1.9 | -1.8 | -1.6 | -1.5 | -1.3 | -1.1 | -1.0 | -0.8 | -0.3 | -0.1 | 0.1 | 0.4 | 0.7 | 0.9 | 1.2 | 1.5 | 1.9 | 2.2 | 2.6 | 2.9 | 3.3 | 3.7 | 4.1 | 4.6 |
| 0.2 | -2.6 | -2.5 | -2.5 | -2.4 | -2.3 | -2.2 | -2.1 | -2.0 | -1.9 | -1.7 | -1.6 | -1.4 | -1.3 | -1.1 | -0.9 | -0.7 | -0.3 | 0.0 | 0.2 | 0.5 | 0.8 | 1.0 | 1.3 | 1.7 | 2.0 | 2.3 | 2.7 | 3.1 | 3.4 | 3.9 | 4.3 | 4.7 |
| | -2.5 | -2.5 | -2.4 | -2.3 | -2.2 | -2.1 | -2.0 | -1.9 | -1.8 | -1.7 | -1.5 | -1.3 | -1.2 | -1.0 | -0.8 | -0.6 | -0.2 | 0.1 | 0.3 | 0.6 | 0.9 | 1.2 | 1.5 | 1.8 | 2.1 | 2.5 | 2.8 | 3.2 | 3.6 | 4.0 | 4.4 | 4.9 |
| 0.4 | -2.5 | -2.4 | -2.3 | -2.3 | -2.2 | -2.1 | -2.0 | -1.8 | -1.7 | -1.6 | -1.4 | -1.3 | -1.1 | -0.9 | -0.7 | -0.5 | -0.1 | 0.2 | 0.4 | 0.7 | 1.0 | 1.3 | 1.6 | 1.9 | 2.3 | 2.6 | 3.0 | 3.3 | 3.7 | 4.2 | 4.6 | 5.1 |
| | -2.4 | -2.3 | -2.3 | -2.2 | -2.1 | -2.0 | -1.9 | -1.8 | -1.6 | -1.5 | -1.3 | -1.2 | -1.0 | -0.8 | -0.6 | -0.4 | 0.1 | 0.3 | 0.6 | 0.8 | 1.1 | 1.4 | 1.7 | 2.1 | 2.4 | 2.8 | 3.1 | 3.5 | 3.9 | 4.4 | 4.8 | 5.3 |
| 0.6 | -2.3 | -2.2 | -2.2 | -2.1 | -2.0 | -1.9 | -1.8 | -1.7 | -1.5 | -1.4 | -1.2 | -1.1 | -0.9 | -0.7 | -0.5 | -0.3 | 0.2 | 0.4 | 0.7 | 1.0 | 1.3 | 1.5 | 1.9 | 2.2 | 2.6 | 2.9 | 3.3 | 3.7 | 4.1 | 4.6 | 5.0 | 5.5 |
| | -2.2 | -2.1 | -2.1 | -2.0 | -1.9 | -1.8 | -1.7 | -1.5 | -1.4 | -1.3 | -1.1 | -0.9 | -0.7 | -0.5 | -0.4 | -0.1 | 0.3 | 0.6 | 0.9 | 1.1 | 1.4 | 1.7 | 2.0 | 2.4 | 2.7 | 3.1 | 3.5 | 3.9 | 4.3 | 4.8 | 5.2 | 5.7 |
| 0.8 | -2.7 | -2.7 | -2.6 | -2.5 | -2.4 | -2.3 | -2.2 | -2.1 | -2.0 | -1.9 | -1.7 | -1.6 | -1.4 | -1.3 | -1.1 | -0.9 | -0.5 | -0.2 | 0.0 | 0.3 | 0.5 | 0.8 | 1.1 | 1.4 | 1.7 | 2.0 | 2.4 | 2.7 | 3.1 | 3.5 | 3.9 | 4.3 |
| | -2.7 | -2.7 | -2.6 | -2.5 | -2.5 | -2.4 | -2.3 | -2.2 | -2.0 | -1.9 | -1.8 | -1.6 | -1.5 | -1.3 | -1.1 | -0.9 | -0.5 | -0.3 | -0.1 | 0.2 | 0.5 | 0.7 | 1.0 | 1.3 | 1.6 | 1.9 | 2.3 | 2.6 | 3.0 | 3.4 | 3.8 | 4.2 |
| 1.0 | -2.4 | -2.7 | -2.6 | -2.5 | -2.5 | -2.4 | -2.3 | -2.2 | -2.1 | -1.9 | -1.8 | -1.6 | -1.5 | -1.3 | -1.1 | -1.0 | -0.5 | -0.3 | -0.1 | 0.1 | 0.4 | 0.7 | 0.9 | 1.2 | 1.5 | 1.9 | 2.2 | 2.5 | 2.9 | 3.3 | 3.7 | 4.1 |
| | -2.9 | -2.9 | -2.6 | -2.5 | -2.3 | -2.2 | -2.2 | -2.2 | -2.1 | -1.9 | -1.8 | -1.7 | -1.5 | -1.3 | -1.2 | -1.0 | -0.6 | -0.4 | -0.1 | 0.1 | 0.4 | 0.6 | 0.9 | 1.2 | 1.5 | 1.8 | 2.1 | 2.5 | 2.8 | 3.2 | 3.6 | 4.0 |
| 1.2 | -3.1 | -3.1 | -3.0 | -2.9 | -2.8 | -2.8 | -2.4 | -2.3 | -2.3 | -2.3 | -2.3 | -1.7 | -1.7 | -1.7 | -1.0 | -0.8 | -0.6 | -0.3 | 0.0 | 0.0 | 0.3 | 0.9 | 1.1 | 1.3 | 1.4 | 2.0 | 2.0 | 2.7 | 3.0 | 3.3 | 3.4 | 3.7 |
| | -3.1 | -3.1 | -3.0 | -3.0 | -2.9 | -2.9 | -2.7 | -2.7 | -2.4 | -2.3 | -2.3 | -2.3 | -1.8 | -1.8 | -1.8 | -1.8 | -0.8 | -0.6 | -0.4 | -0.1 | 0.4 | 0.4 | 0.7 | 1.0 | 1.3 | 1.6 | 1.9 | 2.3 | 2.6 | 2.9 | 3.4 | 3.5 |

**Figure 2** Gradient Field of resultant RT deviation from mean value. Negative (Blue) values represent faster velocities compared to mean value. || mean velocity = 0.238 ms−1 || Dimensions 1.3 x 3.2 m. The black outline represents perpendicular cross section of the shooter, ($y_1$ = 0.6). Velocities are achieved with no skipping, α = 100°.

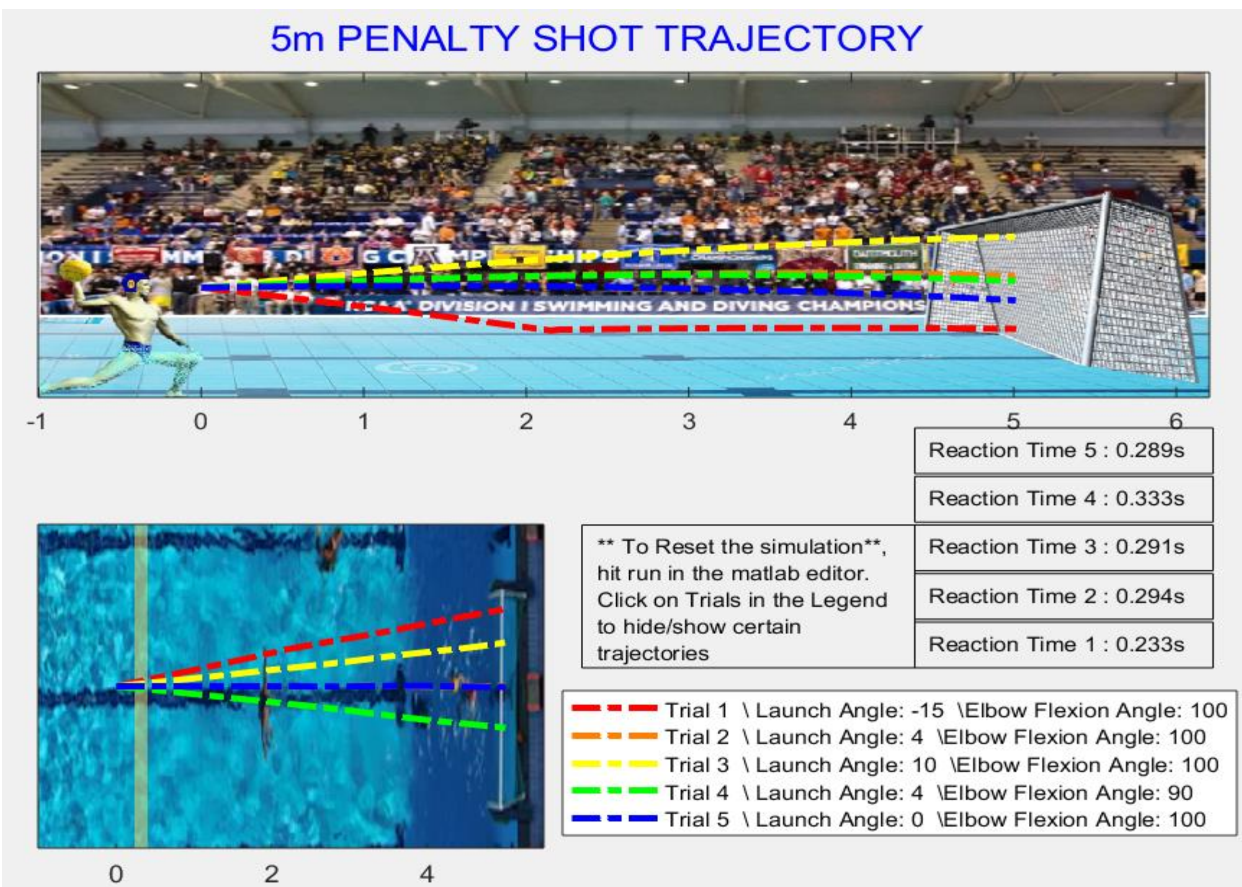


**Figure 3** Simulation output using 5 trajectories at random values.

**Word Count: 1,499**

# 4 References

Abraldes, A. (2012). Throwing Velocity and Efficacy During Water Polo Matches. *The Open Sports Sciences Journal*, 141-145.

Belden, J., Hurd, R., Jandron, M., Bower, A., & Truscott, T. (2015). Elastic spheres can walk on water. *Nature communications*.

Birkhoff, G., Bleick, W., Handler, E., Murnaghan, F., & Smith, T. (1944). Ricochet off water. *A.M.P. Memo. 42.4M*.

Clanet, C. (2015). Sports Ballistics. *Annual Review of Fluid Mechanics*, 455-478.

Dupeux, G., Goff, A., Quéré, D., & Clanet, C. (2010). The spinning ball spiral. *New Journal of Physics*.

Elliot, B., & Armour, J. (1988). The penalty throw in water-polo: A cinematographic analysis. *Journal of Sports Sciences*, 103-114.

Feltner, M., & Nelson, S. (1996). Three-Dimensional Kinematics of the Throwing Arm during the Penalty Throw in Water-polo. *Journal of Applied Biomechanics*, 359-382.

Gardasevic, J., Akpinar, S., Popovic, S., & Bjelica, D. (2019). Increased Perceptual and Motor Performance of the Arms of Elite Water-polo Players. *Applied Bionics and Biomechanics*, 1-10.

Haake, S., Goodwil, S., & Carre, M. (2007). A new measure of roughness for defining the aerodynamic performance of sports balls. *Journal of Mechanical Engineering Science*, 789-806.

Johnson, W., & Reid, S. (1975). Ricochet of Spheres off Water. *Journal of Mechanical Engineering Science*, 71-81.

Melchiorri, G., Padua, E., Padulo, J., Dottavio, S., Cmpagna, S., & Bonifazi, M. (2011). Throwing velocity and kinematics in elite male water-polo players. *The Journal of Sports Medicine and Physical Fitness*, 541-546.

Razak, R., Kee , K., Hussain, R., Kassim, N., & Othman, N. (2018). The effect of hand grip strength and trunk rotation strength on throwing ball velocity. *Movement, Health and Excercise*.

Solum, J. (2017). *RADAR AND THE BIOMECHANICS OF THE SHOT*. Retrieved from Water Polo Planet: http://www.waterpoloplanet.com/radar-and-the-biomechanics-of-the-shot/

Texier, B., Cohen, C., Quere, D., & Clanet, C. (2016). Physics of knuckleballs. *New Journal of Physics*.